

# Description of the Glass Transition by a Percolation Blocking of Local Chemical Order

J. Blétry

C.E.A./C.E.R.E.M./D.E.M., 17, rue des Martyrs, 38054 Grenoble Cedex 9, France

Z. Naturforsch. **51a**, 87–94 (1996); received September 6, 1995

A model for the liquid-glass transition, based on a percolation blocking of local chemical order, is proposed. The case of metallic liquids and glasses, whose structure is dominated by first neighbour chemical arrangement, is first treated. The chemical ordering “reaction” of the liquid phase is studied at thermodynamical equilibrium and the increase of the chemical order parameter with decreasing temperature is calculated. Within a given composition interval, however, a geometrical percolation process is shown to block this reaction below a “percolation temperature” (corresponding to null cooling rate) where the liquid is irreversibly frozen into a glass. The liquid-glass “phase diagram” is established and kinetic arguments, involving “frustrated” finite clusters which are formed close to the percolation threshold, provide an evaluation of the experimentally measured “glass transition temperature” as a function of cooling rate. The validity of this one order parameter model is then discussed with the help of the irreversible thermodynamics theory of Prigogine.

The formation of tetracoordinated glasses is explained by the formation of tetrahedral bonds, when the liquid temperature decreases, and represented by a “hole ordering” reaction. A general description of the structure of tetracoordinated glasses is thus achieved, which applies to amorphous silicon and germanium, III–V compounds, silica, amorphous water etc. Furthermore, an estimation of the temperature interval for the glass transformation of silica is obtained, which agrees well with experiment.

The existence of frustrated clusters gives to glasses a composite structure in the “medium distance order”, which could explain the “fractal nature” of glass fracture surfaces down to the nanometer scale.

**Key words:** Glass transition, Percolation, Short range chemical order, Metallic glasses, Tetracoordinated glasses, Fractography.

## 1. Introduction

Most transitions between bulk phases are dominated by first neighbour interactions (Turnbull [1]). More specifically, the so called glass transition between liquid and glass phases seems to be tightly related with short range chemical order phenomena, which are expressed by the formation of prepeaks in the diffraction patterns (Cahn [2], Bormann and Zöltzer [3], Steeb and Hezel [4], Blétry [5], Lamparter, Sperl, Steeb, and Blétry [6]). On the other hand, amorphization of metallic elements seems to be very difficult, if not impossible (Jäckle [7]), while tetravalent elements, which do exhibit a prepeak in their diffraction patterns (Blétry [8]), can become amorphous.

In order to interpret these facts, we propose a model of the glass transition which is based on a percolation blocking of local chemical order (Blétry [9]). The case of close packed metallic glasses is analyzed from topological, thermodynamical and kinetic points of

view. This model is then extended to loosely packed tetracoordinated systems, proposing a hole ordering representation of their structural evolution. Finally, model involvements in glass fractography are surveyed (Mandelbrot, Passoja, and Paullay [10], Mecholsky [11]).

## 2. Glass Transition in Binary Alloys

### 2.1 Topology

#### 2.1.1. Sticky Hard Sphere Model

The structure of binary liquid or glassy alloys can be represented with good accuracy by close packed random networks of spheres, taking into account atomic size and chemical order effects [5, 8].

In order to represent safely liquid and glassy structures, sphere diameters  $d_1$  and  $d_2$  have to be identified with the first neighbour distances  $d_{11}$  and  $d_{22}$  (which are experimentally determined as the positions of the first maximum in the partial pair distribution functions) and the relation  $d_{12} = \frac{1}{2}(d_{11} + d_{22})$  has to be

Reprint requests to Dr. J. Blétry.

0932-0784 / 96 / 0100-0087 \$ 06.00 © – Verlag der Zeitschrift für Naturforschung, D-72072 Tübingen



Dieses Werk wurde im Jahr 2013 vom Verlag Zeitschrift für Naturforschung in Zusammenarbeit mit der Max-Planck-Gesellschaft zur Förderung der Wissenschaften e.V. digitalisiert und unter folgender Lizenz veröffentlicht: Creative Commons Namensnennung-Keine Bearbeitung 3.0 Deutschland Lizenz.

Zum 01.01.2015 ist eine Anpassung der Lizenzbedingungen (Entfall der Creative Commons Lizenzbedingung „Keine Bearbeitung“) beabsichtigt, um eine Nachnutzung auch im Rahmen zukünftiger wissenschaftlicher Nutzungsformen zu ermöglichen.

This work has been digitalized and published in 2013 by Verlag Zeitschrift für Naturforschung in cooperation with the Max Planck Society for the Advancement of Science under a Creative Commons Attribution-NoDerivs 3.0 Germany License.

On 01.01.2015 it is planned to change the License Conditions (the removal of the Creative Commons License condition “no derivative works”). This is to allow reuse in the area of future scientific usage.

fulfilled [8]. This definition is not completely trivial since these sphere diameters depend on temperature  $T$  and pressure  $P$  (through the dilatation  $\alpha = \frac{1}{V} \frac{\partial V}{\partial T}$  and compressibility  $\chi = -\frac{1}{V} \frac{\partial V}{\partial P}$  coefficients) and account for anharmonic “solid like” effects (Mott and Jones [12]).

The packing fraction  $\gamma$  is then defined as the ratio of the volume of  $N$  spheres to the external volume  $V$ :

$$\gamma = \frac{\pi}{6} \frac{N_1 d_1^3 + N_2 d_2^3}{V} = \frac{\pi}{6} \varrho (c_1 d_1^3 + c_2 d_2^3),$$

where  $N_i$  and  $c_i = N_i/N$  are, respectively, the number and the concentration of spheres belonging to chemical species  $i$  ( $\gamma$  is experimentally derived from measurements of the number density  $\varrho = N/V$ ). According to measurements on ball bearing packings (Scott [13], Lemaignan [14]) and to computer calculations [8],  $\gamma$  is practically independent of the sphere diameter ratio

$$\frac{d_2}{d_1} = 1 + \varepsilon$$

(if  $\varepsilon$  is small, i.e.  $|\varepsilon| \leq 0.5$ ), the atomic concentrations  $c_i$  and the chemical order parameter to be defined later.

In close packed random networks of spheres  $\gamma$  is equal to [13, 14]

$$\gamma_{cp} = 0.637.$$

However, this value depends slightly on “sphere shaking”<sup>1</sup> and is still lacking any mathematical foundation.

On the other hand, and according to the previous definitions, the packing fraction of a glass depends only on its structure and does vary neither with temperature nor with pressure! In practice, the packing fraction of metallic glasses usually lies around 0.70, mainly because the softness of the interatomic pair potentials spreads the first neighbour DIRAC peaks  $\delta(r - d_i)$  over a finite interval and allows diameter “fluctuations” or sphere “overlapping”.

### 2.1.2. Percolation Blocking of Chemical Order

The effect of local chemical order on binary sphere mixtures is mainly characterized by the first neighbour

chemical order parameter<sup>2</sup>:

$$-1 \leq \xi = \frac{\eta_{12} - \eta_{12}^d}{\eta_{12}^d} \leq 1,$$

where  $\eta_{ij}$  is the average number of  $j$  spheres contacting an  $i$  sphere, and  $\eta_{ij}^d$  is the same “partial coordination number” in a chemically disordered mixture (with equal packing fraction and composition).

Conversely, partial coordination numbers can be derived from  $c_i$ ,  $\varepsilon$ , and  $\xi$  by the relations [8]:

$$\begin{aligned} \eta_{11} &= \eta [c_1 (1 - 2\varepsilon c_2) - c_2 (1 + 2\varepsilon c_1) \xi], \\ \eta_{12} &= \eta c_2 [1 + \varepsilon (c_1 - c_2)] (1 + \xi), \\ \eta_1 &= \eta_{11} + \eta_{12} = \eta [1 - \varepsilon c_2 (1 + \xi)], \\ \eta &= c_1 \eta_1 + c_2 \eta_2 \approx 12.6 \gamma, \end{aligned} \quad (1)$$

where  $\eta$  is the overall average coordination number associated with the packing fraction  $\gamma$ , and  $\varepsilon$  is small with respect to 1.

Let us first deal with chemical ordering ( $\xi > 0$ ) in equal size ( $\varepsilon = 0$ ) sphere mixtures. Spheres 1 (“white”) are then preferentially surrounded by spheres 2 (“black”). The average neighbourhood of a 1 sphere can be represented by unique “grey” partners whose chemical nature or “grey level”

$$\lambda_2 = \frac{\eta_{12}}{\eta_1} = c_2 (1 + \xi) \quad (2)$$

lies in the interval  $1 \geq \lambda_2 \geq 0$  (Figure 1).

The chemically ordered “black and white” liquid is then equivalent to a “totally” ordered fictitious mixture where white spheres are exclusively surrounded by grey spheres<sup>3</sup> with fictitious concentrations

$$\begin{aligned} c'_1 &= \frac{\lambda_2 - c_2}{\lambda_2} = \frac{\xi}{1 + \xi} = 1 - c'_2, \\ \eta'_{11} &= 0. \end{aligned} \quad (3)$$

If chemical order develops, i.e. if  $\xi$  increases, the concentration  $c'_1$  of fictitious white spheres increases and they get closer and closer, while their grey partners become darker and darker. However, this ordering process only works till one reaches the site percolation

<sup>2</sup> In the case of heteroatomic attraction, where  $\xi$  is positive, it is not necessary to introduce next neighbour chemical order parameters since their intervals of variation are strongly restricted if  $\xi$  is known (because 2nd ...  $n$ th neighbours may be considered as 1st neighbours of the 1st ...  $(n-1)$ th neighbours).

<sup>3</sup> In this approximation the fluctuations of the neighbourhood or each chemical component are neglected.

<sup>1</sup> Luke Gospel, VI, 38 (between 40 and 90 AC).

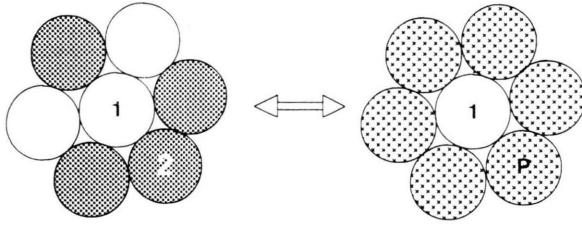


Fig. 1. Conversion of a fluctuating neighbourhood made of black and white spheres into an equivalent average neighbourhood of grey spheres in "total" chemical order.

threshold where an infinite cluster of contacting white spheres is formed. The fictitious packing fraction  $\gamma'_1$  of white spheres is then equal to the (structurally invariant) packing fraction of the site percolation threshold in three dimensions  $p$  (Zallen [15]), i.e.

$$\gamma'_1 = c'_1 \gamma = p = 0.155, \quad (4)$$

and the order parameter  $\xi$  reaches its maximum value [8]<sup>4</sup>

$$\xi_p = \frac{p}{\gamma - p}. \quad (5)$$

According to our model this percolation blocking of local chemical order is responsible for the glass transition.

### 2.1.3. Glass Forming Phase Diagram

The percolation blocking process only works in the interval where white spheres meet "strictly grey" partners (while they would like to meet black partners), i.e. when

$$1 > \lambda_2^p \quad \text{or} \quad c_1 > \frac{\xi_p}{1 + \xi_p}.$$

Inverting the roles of 1 and 2 spheres, one similarly obtains

$$c_2 > \frac{\xi_p}{1 + \xi_p}.$$

The glass forming composition range therefore extends over the interval

$$0 < c_{g1} = \frac{\xi_p}{1 + \xi_p} < c_1 < c_{g2} = \frac{1}{1 + \xi_p} < 1. \quad (6)$$

<sup>4</sup> Equations (4) and (5) can also be demonstrated by considering the average partners of black atoms. For example, if white atoms are ordered with black partners, black atoms are ordered with grey partners made from  $p/(\gamma - p)$  white spheres and  $(\gamma - 2p)/(\gamma - p)$  black spheres.

Between 0 and  $c_{g1}$  the sphere mixture may reach the desired maximum order situation where white spheres are only surrounded by black spheres, i.e.  $\eta_{11} = 0$  and  $\xi_m = \frac{c_1}{c_2}$ , and there is no glass transition. Obviously metallic elements, which cannot undergo such a chemical ordering process, are excluded from the glassy composition interval<sup>5</sup>. The present model could therefore explain why they are so difficult, if not impossible [7], to amorphize.

These results are summarized in Fig. 2, which displays the "liquid-glass transition" surface as a function of  $\gamma$ ,  $c_1$ , and  $\xi$ .

Equation (6) can be extended (with care) to sphere mixtures with size effect [8]. One then obtains the generalized expression of the unsymmetrical composition interval for glass formation:

$$\frac{\xi_p}{1 + \xi_p} \left[ 1 + \frac{2\varepsilon}{1 + \xi_p} \right] < c_1 < \frac{1}{1 + \xi_p} \left[ 1 + 2\varepsilon \frac{\xi_p}{1 + \xi_p} \right]. \quad (7)$$

Relation (7) could account for the few glass forming phase diagrams measured on metallic glasses [3].

## 2.2 Thermodynamics

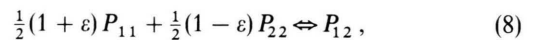
### 2.2.1. Short Range Chemical Ordering in (Metastable) Undercooled Liquids

Let us now calculate the variations of the first neighbour chemical order parameter with temperature in an (undercooled) liquid in (metastable) thermodynamical equilibrium.

If the alloy is represented by a close packed sphere mixture, the total number of pairs per unit volume  $\mathcal{N}$  (at constant pressure) is given by

$$\begin{aligned} \frac{\mathcal{N}}{V} &= \frac{N_{11} + N_{22} + N_{12}}{V} \\ &= \frac{N(c_1 \eta_{11} + c_2 \eta_{22} + 2c_1 \eta_{12})}{2V} = \frac{3\eta\gamma}{\pi d_1^3} (1 - 3\varepsilon c_2), \end{aligned}$$

where  $N_{ij}$  is the number of atomic pairs  $P_{ij}$ , and does not depend on  $\xi$ . Therefore the chemical ordering process can be described by the equilibrium reaction between atomic pairs



<sup>5</sup> Since a percolation blocking of the ordering of subatomic size holes, which subsist in a close packed arrangement, is very unlikely, in contrast with the case of atomic size holes which exist in tetracoordinated glasses.

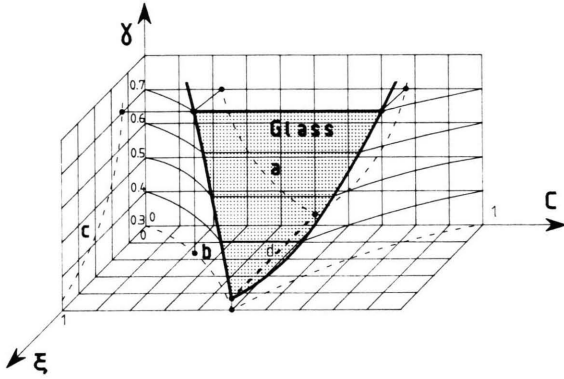


Fig. 2. Geometrical "phase diagram" of the liquid glass transition for  $\varepsilon = 0$ .

Projections  $\begin{cases} (c, \gamma) \\ (\xi, c) \\ (\xi, \gamma) \end{cases}$     Curves  $\begin{cases} (a) c = p/\gamma \\ (b) \xi = c/(1-c) \\ (c) \xi = p/(\gamma-p) \end{cases}$

Line: (d)  $c = 0.5, \gamma = 2p$ .

where the sterical factors  $1 + \varepsilon$  and  $1 - \varepsilon$  account for the atomic size difference. This first order "gas approximation" neglects the interactions between first neighbours of a given atom but is quite sufficient for our purpose (Bethe [16]).

If  $V_{ij}$  represents the potential interaction energy of  $i-j$  pairs and all other energy contributions (like vibration energies which do not vary significantly upon ordering) are neglected, application of the law of mass action to reaction (8) gives

$$\frac{N_{12}}{\sqrt{N_{11}N_{22}}} = \frac{2}{x}, \quad (9)$$

where the size difference has been neglected ( $\varepsilon = 0$ ) and the entropy factor 2 takes into account the respective symmetries of 11, 22 and 12 pairs (Rocard [17]),

$$x = \exp\left(-\frac{V}{k_B T}\right),$$

and

$$V = \frac{1}{2}(V_{11} + V_{22}) - V_{12}$$

is the driving energy difference for chemical ordering.

A straightforward calculation then leads to the relation

$$\xi(T) = \frac{1 - 2c_1c_2(1-x^2) - \sqrt{1 - 4c_1c_2(1-x^2)}}{2c_1c_2(1-x^2)}, \quad (10)$$

which becomes identical with Bethe's [16] classical

relation  $\xi = \frac{1-x}{1+x}$  for  $c_1 = c_2 = 0.5$ .

Figure 3 displays the "bell shape" of this equilibrium  $\xi$  versus  $T$  curve. When the liquid cools down,  $\xi$  increases from 0 up to  $\xi_m = \frac{c_1}{c_2}$ ,  $\xi_m$  being the maximum value which would be reached at  $T = 0$  if there were no geometrical hindrance.

### 2.2.2. Percolation Temperature

If the composition lies in the glass forming composition interval (7), the chemical order parameter of the (metastable) equilibrium liquid should follow (10) upon cooling, down to the percolation temperature  $T_p$  defined by [(5) and Figure 3]

$$\xi(T_p) = \frac{p}{\gamma(T_p) - p}, \quad (11)$$

where an infinite cluster of contacting white spheres is formed. Below  $T_p$ ,  $\xi$  should then remain locked at  $\xi_p$  in an out of equilibrium glassy state.

In contrast with the free volume percolation theory (Cohen and Grest [18]), this process works even in the case where the liquid expands upon glass formation (silica: Douglas and Isard [19], water: Davies and Jones [20]) because it only relies on the intersection of the curves  $\xi(T)$  and  $\frac{p}{\gamma(T) - p}$ .

However, this sharp transition at  $T_p$  cannot be observed because it requires an infinitely slow cooling rate.

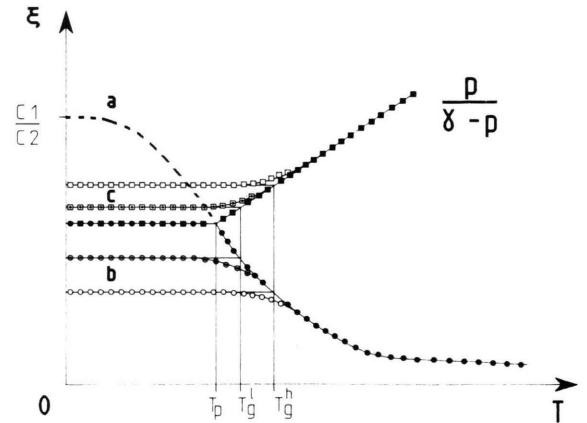


Fig. 3. Determination of the "glass transition temperature": a)  $\xi(T)$  curve of an equilibrium liquid (for  $c = 0.5$ ); b)  $\xi(T)$  curves of a glass forming system at different cooling rates ( $\bullet$ )  $R = 0$ , ( $\circ$ )  $R$  low, ( $\square$ )  $R$  high; c)  $p/[\gamma(T) - p]$  curves of a glass forming system at different cooling rates ( $\blacksquare$ )  $R = 0$ , ( $\square$ )  $R$  low, ( $\circ$ )  $R$  high.

## 2.3 Kinetics

### 2.3.1. Glass Transition Temperature

In practice a liquid glass transformation interval depending on the cooling rate  $R = \frac{dT}{dt}$  is observed around a so called glass transition temperature  $T_g > T_p$ .

In order to describe this process qualitatively, it is convenient to use the equivalent fictitious mixture of white and grey spheres in total chemical order introduced in Section 2-1-2 (since thermodynamical ordering effects are simply taken into account through the grey level parameter).

At high temperature in the equilibrium liquid, the order parameter  $\xi$  and the fictitious white sphere concentration are small ((10) and (3)). The liquid is then represented by a diluted solution of “surrounded atoms” (made of a central white sphere or “singlet” exclusively surrounded by grey spheres (Mathieu, Durand, Bonnier [21])) in a sea of grey spheres.

As the liquid cools down, its order parameter increases together with the concentration of surrounded atoms (3). Therefore the time to reach thermodynamical equilibrium is longer because it requires a “search” for the few configurations avoiding contact between white spheres, in order to preserve the total chemical order between white and grey spheres.

Finally, when approaching the percolation temperature, white spheres become “overcrowded”. During the search for thermodynamical equilibrium (and like in all percolation processes) finite clusters of contacting white spheres are formed for entropical (or geometrical) reasons. These clusters are chemically frustrated, and their formation strongly reduces the atomic diffusion coefficients (because atoms prefer to move between energetically favoured singlet sites). The system then leaves thermodynamical equilibrium, and its chemical ordering rate  $\frac{d\xi}{dt}$  rapidly decreases

until it is frozen at a “glass transition temperature”  $T_g$  into an out of equilibrium state with an order parameter value  $\xi_g$  lower than  $\xi_p$  and an average frustrated cluster size  $l_a(T_g)$  (Figure 3). This model-glass therefore looks like a “nanometric composite” of “frustrated clusters” dispersed into a homogeneous matrix of surrounded atoms.

The corresponding glass transition temperature is defined as the temperature of the (fictitious) liquid in

equilibrium at  $T_g > T_p$  with an order parameter  $\xi(T_g) = \xi_g$  (Figure 3).

### 2.3.2. Cooling Rate Dependence of the Glass Transition Temperature

When the cooling rate increases, the undercooled liquid deviates from equilibrium at higher temperatures and the glass transition temperature is higher. The final cluster size of the glass is then smaller (because these clusters are formed at temperatures farther from  $T_p$ ), and the chemical diffusion coefficient of the glass at low temperature (i.e. for  $T < T_g$ ) is therefore larger.

An order of magnitude estimate of the variations of  $T_g$  with the cooling rate  $R$  can be obtained if one remembers that the chemical ordering reaction (8) requires a permutation of 1 and 2 atoms over a first neighbour distance  $d_{12}$ . Therefore, the system should freeze at a temperature:  $T_g$  fulfilling relation

$$D_1(T_g)\tau \approx d_{12}^2,$$

where  $D_1$  is the interdiffusion coefficient of (both) liquid components,  $\tau = \frac{\Delta T_t}{R}$  is the time interval available for an atomic permutation and  $\Delta T_t$  is the glass “transformation temperature interval” where clusters are evolving. Assuming that  $D_1$  follows an Arrhenius law

$$D = D_{10} \exp\left(-\frac{V_1}{k_B T}\right),$$

one finally obtains

$$R = \frac{D_1(T_g)\Delta T_t}{d_{12}^2} = R_o \exp\left(-\frac{V_1}{k_B T_g}\right) \quad (12)$$

with

$$R_o = \frac{\Delta T_t D_{10}}{d_{12}^2}.$$

For moderate cooling rates,  $\Delta T_t$  does not vary too much and (12) agrees with empirical relations which give a  $\log R$  dependence for  $\frac{1}{T_g}$  ([7], Zarzycki [22], Owen [23]).

### 2.3.3. Transformation Interval of Metallic Glasses

The glass transformation interval can only be calculated from (12) in the very few cases where  $D_1(T_g)$ ,  $d_{12}$ , and  $R$  are known.



However, the case of Ni-B metallic glasses, whose chemical ordering has been proved by neutron diffraction experiments [6], allows (12) to be checked. Using the diffusion coefficient of boron:  $D_B(T_g) \approx 10^{-12} \text{ cm}^2 \text{ s}^{-1}$ , which has been measured in the analogous metal-metalloid glasses Fe-Ni-B (Cahn, Evetts, Patterson, Somekh, and Kenway-Jackson [24]), a nickel-boron distance of  $d_{\text{Ni-B}} = 2.1 \cdot 10^{-8} \text{ cm}$  and a typical cooling rate of  $R \approx 10^5 \text{ K s}^{-1}$ , one finds a glass transformation interval  $\Delta T_i \approx$  a few 10 K, which agrees satisfactorily with experimental observations on metallic glasses (Chen [25]).

#### 2.3.4. Discussion Based on Irreversible Processes Thermodynamics

The present model gives a simple physical meaning to the extensive order parameter  $\Xi$  introduced by Prigogine and Defay [26] in their description of the irreversible glass transition. Rewriting reaction (8) as

$$-2 \frac{dN_{11}}{1 + \varepsilon} = -2 \frac{dN_{22}}{1 - \varepsilon} = dN_{12} = d\Xi,$$

$\Xi$  may be identified by

$$\Xi = N_{12}^d \xi, \quad (13)$$

where

$$N_{12}^d = N \eta c_1 c_2 [1 + \varepsilon(c_1 - c_2)]$$

is the number of 1–2 pairs in a chemically disordered mixture.

According to Prigogine and Defay [26], our one order parameter theory provides a good description of the glass transition if the condition

$$\Delta\chi \Delta C_p = VT \Delta\alpha^2 \quad (14)$$

is fulfilled, where  $\Delta\chi$ ,  $\Delta C_p$ , and  $\Delta\alpha$  are respectively the differences between the liquid and the glass compressibilities, specific heats and dilatation coefficients around  $T_g$ .

Since condition (14) is seldom fulfilled, many authors have introduced a spectrum of order parameters ([20, 25], Gardon and Narayanaswamy [27]) to interpret the experimental results more accurately. The present model could also be improved either by taking into account the cluster size distribution or by introducing next neighbour order parameters.

### 3. Glass Transition in Tetravalent Compounds

#### 3.1 Hole Ordering

At first sight it would seem that the glass transition in loosely packed tetracoordinated glasses [amorphous elements (silicon, germanium), silicate, fluoride and phosphate glasses, amorphous ice, etc.] cannot be interpreted within the preceding framework.

However, it was shown in [8] that the formation and “rigidification” of tetrahedral bond angles (when the temperature of the corresponding liquids decreases<sup>6</sup>) can be represented, to a good approximation, by a chemical ordering process between atoms and spherical holes in close packed arrangement. The regular intercalation of holes between atoms then leads to the formation of tetrahedral bond angles (Figure 4).

In tetracoordinated systems, the glass transition can therefore be interpreted as a percolation blocking of the ordering reaction between atoms and holes.

If the packing fraction of this hole-atom glass is

$$\gamma_{\text{th}}^g \approx \gamma_{\text{cp}} = 0.637 \approx 4p,$$

its average coordination number, (1) and hole-atom order parameter, (5), are respectively given by

$$\eta_{\text{th}}^g = 8.0$$

and

$$\xi_{\text{th}}^g = 0.32.$$

#### 3.2 Structure of Amorphous Tetravalent Elements

##### 3.2.1. Model of Tetracoordinated Glasses

In the most simple case of tetravalent elements, and by analogy with their cubic diamond crystalline structure, one may assume that atoms and holes have identical diameters and concentrations. The atomic packing fraction of these glasses is then given by

$$\gamma_t^g = 0.5 \gamma_{\text{th}}^g = 0.32 \approx 2p,$$

i.e. very close to the cubic diamond value

$$\gamma_{\text{cd}} = \frac{\pi\sqrt{3}}{16} = 0.34,$$

<sup>6</sup> The flexibility of the bond angle in tetracoordinated liquids explains why they are denser than the corresponding crystalline phases whose bond angle is rigidly locked at 109°47' (Si, Ge, III–V compounds, etc.). Conversely, the “rigidification” of bond angles, (or the ordering of atomic holes), which is responsible for the prepeak increase in the diffraction patterns, explain why the liquid water density decreases with decreasing temperature below 4°C.

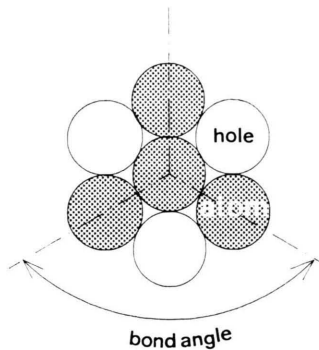


Fig. 4. Preservation of bond angles by ordered holes in tetravalent glasses.

and their atomic coordination number is close to

$$\eta_t^g = 4.0,$$

as it should be for tetravalent elements.

This tetracoordinated glassy network is probably very close to the Zachariesen [28] and Polk [29] poly-tetrahedral network. However, the explicit introduction of holes allows the glass transition to be related to the structural evolution.

### 3.2.2. Amorphous Silicon and Germanium

Model and experimental densities, coordination numbers and structure factors of amorphous silicon (Moss and Graczyk [30]) and germanium (Etherington, Wright, Wenzel, Dore, Clarke, and Sinclair [31]) do not differ by more than 10% [8]. The rustic hole-atom model therefore provides a first approximation for the structural description of tetracoordinated systems.

### 3.3 Structure of Amorphous III–IV Compounds

In analogy with their zinc blende crystal structure, where first neighbour pairs are exclusively III–V heteroatomic pairs, the glassy structure of III–V compounds may be described by a chemically ordered arrangement of III and V atoms on the tetracoordinated amorphous network. Beside the order parameter  $\xi_{th}^g$  (which describes the hole-atom arrangement, responsible for the tetravalent bond formation), a second order parameter  $\xi_{III-V}^g$  has therefore to be introduced for the description of the III and V atoms arrangement on the tetracoordinated network with packing fraction  $\gamma_t^g = 2p$ . Relation (5) then shows that

this order parameter is close to

$$\xi_{III-V}^g - \nu \approx 1.$$

The glass forming composition interval is thus reduced to exact stoichiometry (cf. (6)):

$$c_{III}^g \approx c_V^g \approx 0.5,$$

since only two partial networks with packing fraction  $p$  can percolate simultaneously. This severe requirement could account for the problems encountered in the elaboration of homogeneous III–V glasses far from stoichiometry (Dixmier, Gheorghiu, Theye [32]).

On the other hand, the prepeak which is associated with the chemical ordering of III and V atoms should be superposed with the hole-atom ordering prepeak, since the atom III-atom V and hole-atom first neighbour distances are equal.

### 3.4 Transformation Interval of Silica

In the high temperature crystalline phases of silica (cristobalite and tridymite), silicon atom tetrahedra are formed which delimit atomic size “cages” (Soules [33]). In glassy silica one therefore expects that silicon atoms will form the tetracoordinated amorphous network described in section 2-2-1 (one does not consider here the traditional  $\text{SiO}_4$  tetrahedra!).

X-ray diffraction measurements performed by Leadbetter and Wright [34] on the chemically homologous system  $\text{GeO}_2$  confirm this model. In that case, the diffracted intensity is dominated by the contribution of germanium atoms and practically identical (within a similarity transformation) with the structure factor of the tetracoordinated amorphous network.

A numerical estimation of the temperature interval for the glassy transformation of pure silica may therefore be derived from (12). Using the Brebec, Seguin, Sella, Bevenot, and Martin measurements [35] of the silicon diffusion coefficient  $D_{Si}(T_g) \approx 10^{-18} \text{ cm}^2 \text{ s}^{-1}$  at  $T_g \approx 1200^\circ\text{C}$  and the silicon-hole (or silicon-silicon) distance  $d_{\text{Si-Hole}} = 3.2 \times 10^{-8} \text{ cm}$ , one obtains, for a typical cooling rate of  $0.1 \text{ K s}^{-1}$ , a transformation interval width  $\Delta T_t \approx 100 \text{ K}$ , which is in rather good agreement with industrial practice.

## 4. Fractography

The “fractal nature” [11] of glass fracture surfaces down to the nanometer scale can be directly inferred from the percolation process underlying the glass

transition. More precisely, it may be assumed that the glass composite structure described in Section 2-3-1 will be revealed by fracture surfaces, since "chemically frustrated clusters" should have a lower mechanical strength than the matrix made of "chemically satisfied surrounded atoms". The size of nanometric "islands" observed by atomic force microscopy on the mirror zone of fracture surfaces (Creuzet and Guilloteau [36]), or by high resolution electron microscopy on silica fiber tips (Ajayan and Sumio Iijima [37]), could thus be identified with the average size of frustrated clusters  $l_a(T_g)$ .

The cluster size can also be connected to the "characteristic length" or "fractal generator  $a_0$ " which relates the mechanical properties (elastic modulus, fracture energy) with the roughness or the "fractal dimension  $d^*$ " of glass fracture surfaces [11]. In particular, it should be interesting to study the variations of  $a_0$  and  $d^*$  with the cooling rate  $R$  which determines the glass transition temperature and the average cluster size. According to the present model  $a_0$  and  $d^*$  should increase with decreasing cooling rate. The fractal law followed by glass fracture surfaces could then be justified from the nanometer to the macroscopic scale, since it is well known that tempered glass breaks

into smaller pieces than annealed glass, because of the differences in stress distribution, but also because of "structural inhomogeneities" (Acloque [38], Gardon [39]).

## 5. Conclusion

It has been shown here that the glass transition in metallic and tetracoordinated glasses can be explained by a percolation blocking of local chemical order upon cooling. This percolation model can also explain the fractal shape of the glass fracture surfaces down to nanometric distances.

On the other hand, this description could likely be extended to all glassy systems where a short range chemical order condition has to be respected. For example, ionic bonding glasses should also be studied in that way, using a non additive distance model for their structural representation [8].

## Acknowledgements

Thanks are due to Dr. J. Brown, Pr. J. Friedel and Prof. S. Steeb for helpful suggestions during the preparation of this paper.

- [1] D. Turnbull, *Solid State Physics* **3**, 226 (1956) Academic Press.
- [2] R. W. Cahn, *J. de Physique, Colloque C9, Sup. 12*, **43**, 55 (1982).
- [3] R. Bormann and K. Zöltzer, *Phys. Stat. Sol. A* **131**, 69 (1992).
- [4] S. Steeb and R. Hezel, *Z. Metallk.* **57**, 374 (1966).
- [5] J. Blétry, *Z. Naturforsch.* **33a**, 327 (1979).
- [6] P. Lamparter, W. Sperl, S. Steeb, and J. Blétry, *Z. Naturforsch.* **37a**, 1223 (1982).
- [7] J. Jäckle, *Rep. Prog. Phys.* **49**, 171 (1986).
- [8] J. Blétry, *Phil. Mag.* **B 62**, 469 (1990).
- [9] J. Blétry, *Note technique CEA CENG/DEM 44*, (1992).
- [10] B. B. Mandelbrot, D. E. Passoja, and A. J. Paullay, *Nature London* **308**, 721 (1984).
- [11] J. J. Mecholsky, *Proc. 17th Int. Congress on Glass* **5**, (Pekin, 10/1995), p. 473.
- [12] N. F. Mott and H. Jones, *Theory of the properties of metals and alloys*, Oxford Univ. Press, Oxford 1936.
- [13] J. D. Scott, *Nature London* **188**, 908 (1960).
- [14] C. Lemaignan, *Acta Met.* **28**, 1657 (1980).
- [15] R. Zallen, *The Physics of amorphous solids*, John Wiley, New York 1983.
- [16] A. Bethe, *Proc. Roy. Soc. A London* **150**, 552 (1935).
- [17] Y. Rocard, *Thermodynamique 2ème édition*, Ed. Masson, (1967).
- [18] M. H. Cohen and G. S. Grest, *Phys. Rev. B* **20**, 1077 (1979).
- [19] R. W. Douglas and J. O. Isard, *J. Soc. Glass. Techn.* **35**, 206 (1951).
- [20] R. O. Davies and G. O. Jones, *Adv. Phys.* **2**, 370 (1953).
- [21] J. C. Mathieu, F. Durand, and E. Bonnier, *J. Chim. Phys.* **62**, 88 (1965).
- [22] J. Zarzycki, *Les verres et l'état vitreux*, Masson Ed. (1982).
- [23] A. E. Owen, *Amorphous solids and the liquid state*, Plenum Press, March. Street, Tosi, 395 (1985).
- [24] R. W. Cahn, J. E. Evetts, J. Patterson, R. E. Somekh, and C. Kenway Jackson, *J. Mater. Sci.* **15**, 702 (1980).
- [25] H. S. Chen, *Glass science and technology*, **3**, Uhlmann, Kreidl Ed., Academic Press, London 1986, p. 181.
- [26] I. Prigogine and R. Defay, *Thermodynamique chimique*, Ed. Desoer, Liège 1950.
- [27] R. Gardon and O. S. Narayanaswamy, *J. Amer. Soc.* **53**, 380 (1970).
- [28] W. H. Zacharysen, *J. Amer. Soc.* **54**, 3841 (1932).
- [29] D. E. Polk, *J. Non Cryst. Sol.* **5**, 365 (1971).
- [30] S. C. Moss and J. F. Graczyk, *Phys. Rev. Let.* **23**, 1167 (1969).
- [31] G. Etherington, A. C. Wrigth, J. T. Wenzel, J. C. Dore, J. H. Clarke, and R. N. Sinclair, *J. Non Cryst. Sol.* **48**, 265 (1982).
- [32] J. Dixmier, A. Gheorghiu, and M. L. Theye, *J. Phys. C* **17**, 2271 (1984).
- [33] T. F. Soules, *Glass Science and Technology*, **4A**, Uhlmann, Kreidl Ed., Academic Press, London 1990, p. 267.
- [34] A. J. Leadbetter and A. C. Wright, *J. Non Cryst. Sol.* **7**, 37 (1972).
- [35] G. Brebec, R. Seguin, C. Sella, J. Bevenot, and J. C. Martin, *Acta Met.* **28**, 327 (1980).
- [36] F. Creuzet and E. Guilloteau, *Proc. 17th Int. Congress on Glass* **1**, 13 (Pekin 10/1995).
- [37] P. M. Ajayan and Sumio Iijima, *Phil. Mag. Let.* **65**, 43 (1992).
- [38] P. Acloque, *Verres Réfract.* **5**, 247 (1951).
- [39] R. Gardon, *Glass Science and Technology*, **5**, Uhlmann, Kreidl Ed., Academic Press, London 1980, p. 145.